

# Journal of Materials Chemistry C

Accepted Manuscript



This is an *Accepted Manuscript*, which has been through the Royal Society of Chemistry peer review process and has been accepted for publication.

*Accepted Manuscripts* are published online shortly after acceptance, before technical editing, formatting and proof reading. Using this free service, authors can make their results available to the community, in citable form, before we publish the edited article. We will replace this *Accepted Manuscript* with the edited and formatted *Advance Article* as soon as it is available.

You can find more information about *Accepted Manuscripts* in the [Information for Authors](#).

Please note that technical editing may introduce minor changes to the text and/or graphics, which may alter content. The journal's standard [Terms & Conditions](#) and the [Ethical guidelines](#) still apply. In no event shall the Royal Society of Chemistry be held responsible for any errors or omissions in this *Accepted Manuscript* or any consequences arising from the use of any information it contains.

**Ultrafast Chemical Dynamic Behavior in Highly Epitaxial LaBaCo<sub>2</sub>O<sub>5+δ</sub> Thin Films**

H. B. Wang,<sup>1,2†</sup> S. Y. Bao,<sup>1†</sup> J. Liu,<sup>1</sup> G. Collins,<sup>1</sup> C. R. Ma,<sup>1</sup> M. Liu,<sup>1,3</sup> C. L. Chen,<sup>1,4\*</sup> C. Dong,<sup>2</sup>  
M.-H. Whangbo,<sup>5</sup> H. M. Guo,<sup>6</sup> and H. J. Gao<sup>6</sup>

<sup>1</sup> Department of Physics and Astronomy, University of Texas at San Antonio, TX 78249

<sup>2</sup> School of Materials Science and Engineering, Dalian University of Technology, Dalian  
116024, China

<sup>3</sup> Electronic Materials Research Laboratory, Xi'an Jiaotong University, Xi'an 710049, P. R.  
China

<sup>4</sup> The Texas Center for Superconductivity, University of Houston, Houston, Texas 77204

<sup>5</sup> Department of Chemistry, North Carolina State University, Raleigh, North Carolina  
27695-8204

<sup>6</sup> Institute of Physics, Chinese Academy of Sciences, Beijing 100080, China

† Wang and Bao contributed equally to this work.

\* Author to whom correspondence should be address: Electronic address: [cl.chen@utsa.edu](mailto:cl.chen@utsa.edu)

PACS numbers:

**Abstract**

The redox reactions of highly epitaxial  $\text{LaBaCo}_2\text{O}_{5+\delta}$  (LBCO) thin films exposed to the switching flow of reducing ( $\text{H}_2$ ) and oxidizing ( $\text{O}_2$ ) gases were examined at various temperatures between 260 – 700 °C by measuring their electrical resistance using a precise ac bridge measurement system. The as-grown LBCO films have very good electrical conductivity at low/medium temperatures between 400 – 700 °C, and are extremely sensitive to the reducing/oxidizing environments with superfast redox dynamics. The LBCO thin films show more complex redox reactions at low temperatures (300 – 350 °C) suggesting the occurrence of conducting-to-insulating-to-conducting transitions during the redox reactions. In particular, the insulating-to-conducting transition under oxidation process is superfast with the largest resistance change of up to  $3 \times 10^7 \Omega/\text{s}$  even at low temperature of 300 °C. The extremely short response time, the giant resistance change, and the excellent chemical stability in a broad temperature range of 260 – 700 °C suggests that the highly epitaxial LBCO thin-film can be an excellent candidate for low-temperature solid oxide fuel cells, chemical sensors, and catalyst applications.

**Keywords:**  $\text{LaBaCo}_2\text{O}_{5+\delta}$ ; epitaxial thin film; mixed conductor; redox reaction; gas sensor; catalyst

## 1. Introduction

Recently the 112-type cobalt oxides  $\text{LnBaCo}_2\text{O}_{5.5}$  (LnBCO) (Ln = rare earth) with perovskite structure have become a subject of intense studies, both theoretically and experimentally, due to their unusual magnetic and electrical transport properties suitable.<sup>1,2,3,4</sup> The structure of the double-perovskite  $\text{LnBaCo}_2\text{O}_{5+\delta}$  has the layer sequence of  $[\text{LnO}_\delta]$   $[\text{CoO}_2]$   $[\text{BaO}]$   $[\text{CoO}_2]$  along the  $c$  axis. With the ideal oxygen stoichiometry of 5.5 per formula unit (i.e.,  $\delta = 0.5$ ), the average oxidation state of Co is +3.  $\text{LnBaCo}_2\text{O}_{5+\delta}$  with different extents of oxygen deficiency gives rise to ordered, nano-ordered, and disordered phases. The ionic/electronic conductivities of  $\text{LnBaCo}_2\text{O}_{5+\delta}$  depend on the extent of oxygen deficiency thereby leading to a family of mixed ionic/electronic conducting materials with different physical/chemical properties.<sup>5,6,7,8,9,10</sup> Taskin et al. observed that the A-site ordered  $\text{GdBaCo}_2\text{O}_{5.5+\delta}$  significantly enhances oxygen diffusivity.<sup>11</sup> The previous studies found that the A-site ordered  $\text{PrBaCo}_2\text{O}_{5.5+\delta}$  exhibits ultrafast oxygen transport kinetics at low temperatures ranging 300 – 500 °C.<sup>12,13,14</sup> The size difference between  $\text{La}^{3+}$  and  $\text{Ba}^{2+}$  is small, which makes it difficult for the  $\text{La}^{3+}$  and  $\text{Ba}^{2+}$  ions to order, but the ordered 112-type  $\text{LaBaCo}_2\text{O}_{5+\delta}$  (LBCO) can be prepared under specific synthesis conditions. Rautama et al. successfully fabricated and characterized the nanoscale-ordered and disordered forms of the fully oxidized  $\text{LaBaCo}_2\text{O}_6$  as well as the ordered form of the oxygen-deficient  $\text{LaBaCo}_2\text{O}_{5.5}$ .<sup>15,16</sup> With different synthesis methods, many studies have found that the oxygen content in the Ln/Ba ordered perovskites  $\text{LnBaCo}_2\text{O}_x$  can be varied from  $x = 6$  to  $x = 4.5$ , which leads to a change of the average cobalt oxidation state from +3.5 to +2.<sup>17,18</sup> In addition, Seddon et al. found the ground samples of  $\text{YBaCo}_2\text{O}_5$  and  $\text{LaBaCo}_2\text{O}_5$  are reduced by a strong reductant NaH to form  $\text{YBaCo}_2\text{O}_{4.5}$  and  $\text{LaBaCo}_2\text{O}_{4.25}$ , respectively.<sup>19</sup> Recently, we

have successfully obtained the highly epitaxial LnBCO thin films and systematically studied the epitaxial nature and their electrical transport, magnetic and chemical properties.<sup>20,21,22,23,24,25,26,27,28</sup> When these films are exposed to the switching flow of reducing (4% H<sub>2</sub> + 96% N<sub>2</sub>, which will be referred to as H<sub>2</sub> for simplicity) and oxidizing (O<sub>2</sub>) gases, their electrical resistance exhibits a ultrafast and dramatic change in a very broad temperature range varying from 400 to 800 °C, which reflects the change in the oxidation states of the cobalt atoms under the different redox environments.<sup>29</sup> In this paper, we carry out resistance measurements on the highly epitaxial LBCO thin films under the switching flow of H<sub>2</sub> and O<sub>2</sub> gases in the temperature range of 260 – 800 °C to find the occurrence of a conducting-to-insulating transition at medium temperatures (400~700 °C) and a conducting-to-insulating-to-conducting transition at lower temperatures (300 and 350 °C). These observations are expected to be of potential importance developing the up-to-date low temperature SOFC cathode, chemical sensors and vehicle exhaust catalyst.

## 2. Experiments

LBCO thin films were epitaxially grown on (001) LaAlO<sub>3</sub> (LAO) single crystal ( $c_{\text{LAO}} = 0.3788$  nm) substrates by using a KrF excimer (a wavelength of 248 nm) pulsed laser deposition (PLD) system. An energy density of 2.0 J/cm<sup>2</sup> and a laser repetition rate of 5 Hz were adopted during the film deposition. A high density, single phase, stoichiometric (LaBa)Co<sub>2</sub>O<sub>5+ $\delta$</sub>  target was purchased from MTI Crystal Inc. Highly epitaxial LBCO thin films were achieved in an optimized growth condition at 850 °C with oxygen pressure of 250 mTorr. The as-grown films were in situ annealed in 200 Torr oxygen for 15 min at 850 °C and

cooled down to room temperature at a rate of 5 °C/min. The microstructure and crystallinity of the as-grown LBCO films were examined by a routing x-ray diffraction technique and characterized by cross sectional and plan-view transmission electron microscopy, details of which are given in the previous reports.**Error! Bookmark not defined.** The chemical dynamic measurements on the LBCO films were conducted by using a Lake Shore 370 AC Precise Resistance Bridge System in the temperatures ranging from 260 to 700 °C under pure oxygen or mixture of 5% hydrogen and 95% nitrogen (H-N mixture) in a pressure of 1 atm. Platinum leads were glued on the film surface with high temperature silver paste, were air-dried at room temperature and were annealed at 800 °C before measurements.

### 3. Results and discussion

#### 3.1. Medium temperature transitions

The ac conductivity measurements indicate that at medium temperatures (400~700 °C), the resistance of the LBCO thin films changes drastically during the redox reactions. Under oxidizing environments of O<sub>2</sub>, the LBCO thin films are good electrical conductors with resistance R less than 1000 Ω. Liu et al. studied the temperature dependence of the electrical resistivity of the LBCO thin films and found the linear relation between  $\ln(\rho/T)$  and  $1/T$ ,**Error! Bookmark not defined.** which corresponds to the resistivity behavior of small polarons.<sup>30</sup> Thus, the conductivity of the LBCO thin films comes from the coexistence of Co<sup>3+</sup> and Co<sup>4+</sup> ion according to the mechanism of small-polaron hopping conduction of most mixed-valence transition metal oxides.<sup>31,32,33</sup> As the gas flow was switched from O<sub>2</sub> to the H<sub>2</sub>, the Co<sup>4+</sup> ions become reduced to Co<sup>3+</sup> ions. As the reduction of the LBCO thin films proceeds,

the amount of  $\text{Co}^{4+}$  decreases directly lowering the amount of small-polarons as carriers and hence raising the resistance of the LBCO thin films. Finally, almost all  $\text{Co}^{4+}$  ions are reduced to  $\text{Co}^{3+}$  ions making the LBCO thin films insulating with resistance greater than  $10^7 \Omega$ . Note that the resistance does not change any more even if the reduction time is increased at medium temperature above  $400^\circ\text{C}$ . This is different from the low temperature ( $260\sim 350^\circ\text{C}$ ) phenomenon (see below). The change in the resistance  $R$  under the switching flow of the reducing/oxidizing gas at  $500^\circ\text{C}$  is shown in **Fig. 1(a)**, and the associated  $dR/dt$  in **Fig. 1(b)**. As the gas flow is switched from  $\text{H}_2$  to  $\text{O}_2$ , the oxidation from  $\text{Co}^{3+}$  to  $\text{Co}^{4+}$  occurs, and the resistance decreases ultrafast with rate much larger than the reduction reaction. This indicates that the reduced LBCO thin films have a large number of oxygen vacancies and  $\text{Co}^{3+}$  ions are extremely sensitive to  $\text{O}_2$ . Furthermore, at  $500^\circ\text{C}$ , the LBCO thin films show excellent chemical stability with good reproducibility of the conducting-to-insulating transitions.

### 3.2. Low temperature transitions

While monitoring the resistance change during the redox reactions at low temperatures ( $260\sim 400^\circ\text{C}$ ), we found that the LBCO thin films go through more complex transitions involving three obvious states with a sudden change in the resistance. Fig. 2 shows the  $R$  vs.  $t$  and  $dR/dt$  vs.  $t$  curves at  $350^\circ\text{C}$ . As shown in Fig. 2(a), there is a peak in the  $R$  vs.  $t$  curve during each reduction cycle under  $\text{H}_2$  and during each oxidation cycle under  $\text{O}_2$ . This phenomenon suggests that each transition between conducting and insulating states in the early part of the reduction reaction cycle is followed by a transition between insulating and conducting states. These transitions are also reversible through the redox reactions. Under the

repetitive switching of the redox environments, the reduction and oxidation processes of the LBCO films are highly reversible as can be seen from **Fig. 2** for the case of the redox reactions at 350 °C. **Fig. 2b** shows that, as the gas flow is switched from O<sub>2</sub> to H<sub>2</sub>, the resistance R of LBCO increases to the maximum value and then decreases gradually to the equilibrium value. As the gas flow is switched from H<sub>2</sub> back to O<sub>2</sub>, the resistance rapidly reaches its maximum value with the maximum rate of  $\sim 10^9$  Ω/s and then quickly decreases to the stable value. These resistance changes are attributed to the average Co oxidation states on the surface of the films. In pure O<sub>2</sub> environment, LBCO can be fully oxidized to become ErBaCo<sub>2</sub>O<sub>6</sub> with the Co average oxidation state of +3.5. As the gas flow changes from O<sub>2</sub> to H<sub>2</sub>, LBCO would be reduced to become LaBaCo<sub>2</sub>O<sub>5</sub>(OH) and then LaBaCo<sub>2</sub>O<sub>5.5</sub> (by losing oxygen in terms of H<sub>2</sub>O) with average Co oxidation state of +3, which explains the sharp increase in the resistance. A further reduction under H<sub>2</sub> would lead LBCO to LaBaCo<sub>2</sub>O<sub>4.5</sub>(OH) and then LaBaCo<sub>2</sub>O<sub>5</sub> with average Co oxidation state of +2.5, which explains the sharp decrease in the resistance.

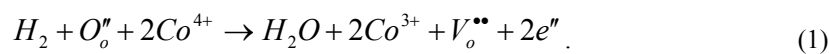
Fig. 3 (a) and (b) show the detailed R vs. t measurements for the reduction and oxidation cycles at various temperatures which indicate that at a given temperature the resistance change of the LBCO films under oxidation is much faster than that under reduction. When the gas flow is switched from H<sub>2</sub> to O<sub>2</sub>, the resistance drops down by a few orders of magnitude, and this change depends sensitively on the temperature. The resistance under O<sub>2</sub> or H<sub>2</sub> is much higher at low temperatures than that at high temperatures. Below  $\sim 400$  °C the reduction under H<sub>2</sub> occurs in one step at high temperatures, but in two steps (i.e., a very sharp increase followed by a gradual decrease).



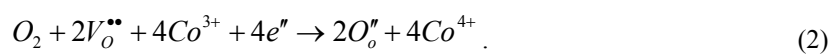
The observed resistance of the LBCO films under the flow of the redox gases can be understood by considering the average Co oxidation state. The resistance should be low when the average Co oxidation state is fractional (e.g., +3.5 and +2.5) because it signals the presence of mixed valence cobalt ions (e.g.,  $\text{Co}^{3+}/\text{Co}^{4+}$  and  $\text{Co}^{2+}/\text{Co}^{3+}$ , respectively) and hence the occurrence of either hopping with low activation energy or metallic conductivity. In contrast, the resistance of the LBCO films should be high when the average Co oxidation state is an integer (e.g., +3 and +2) because electron-hopping is difficult in the case of single valence. The average Co oxidation state is +3.5 for  $\text{LaBaCo}_2\text{O}_6$ , +3 for  $\text{LaBaCo}_2\text{O}_{5.5}$ , and +2.5 for  $\text{LaBaCo}_2\text{O}_5$ . Our first principles density functional theory calculations for  $\text{LaBaCo}_2\text{O}_6$  and various probable structures of  $\text{LaBaCo}_2\text{O}_{5.5}$  and  $\text{LaBaCo}_2\text{O}_5(\text{OH})$  show that hydrogen atoms are present in LBCO as bound to oxygen forming O-H bonds. Then, the average Co oxidation state is +3 for  $\text{LaBaCo}_2\text{O}_5(\text{OH})$ , and +2.5 for  $\text{LaBaCo}_2\text{O}_{4.5}(\text{OH})$ , and +2 for  $\text{LaBaCo}_2\text{O}_{3.5}(\text{OH})_2$ .

### 3.3. Redox equations

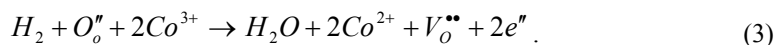
In general, any state transition of the LBCO thin films should arise from the chemical reactions. The reduction reaction of the LBCO thin films corresponding to their conducting-to-insulating transition can be expressed as



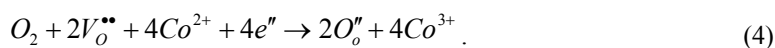
While the oxidation reaction corresponding to the insulating-to-conducting transition can be expressed as



The LBCO thin films are stabilized at the insulating state with  $\text{Co}^{3+}$  ions under  $\text{H}_2$  at medium temperatures, probably because the oxygen potential (i.e., the Gibbs energy of formation  $\Delta G$ )<sup>34</sup> of  $\text{H}_2\text{O}$  is lower than that of the LBCO films with  $\text{Co}^{4+}$  ions but higher than that of LBCO films with  $\text{Co}^{3+}$  ions. However, the oxygen potentials are temperature-dependent, so it is possible that the oxygen potential of  $\text{H}_2\text{O}$  might become lower than that of the LBCO films with  $\text{Co}^{3+}$  ions. In fact, a further reduction reaction of the LBCO thin films following the reaction (1) does continue according to the sudden change in the resistance at low temperatures. The further reduction reaction can be expressed as



As a result of the reaction (3), the LBCO thin films are converted from the insulating to a conducting state, in which new small polarons might play the role of new carriers, as depicted in Fig 2(c). The oxidation reaction corresponding to the semiconducting-to-insulating transition can be expressed as



### 3.4. Analysis of the cycling stability

Usually, changes in the oxygen vacancy concentration of the LBCO thin films are expected to bring about expansion, contraction or even destruction of their structures. Nevertheless, as shown in **Fig. 2(a)** and **Fig. 4(a)**, the transitions among the different states has good reproducibility during five to seven reduction/oxidation cycles at low temperatures. The repeatable R vs. t curves in these cycles reflects a repeatable change in the oxygen vacancy concentration and the variation of the Co oxidation states, and also reveals good stability of the chemical properties of the LBCO thin films under the reducing/oxidizing

environments. The latter may benefit from the stable frame structure of the epitaxial thin films. According to the neutron diffraction studies of Seddon et al.,<sup>19</sup> the  $\text{LaBaCo}_2\text{O}_{4.25}$  prepared by a low-temperature reduction of  $\text{LaBaCo}_2\text{O}_5$  using NaH contains cobalt in three distinct coordination environments, namely,  $\text{CoO}_4$  tetrahedra (50%),  $\text{CoO}_5$  square-pyramids (25%), and  $\text{CoO}_4$  square-planes (25%). Owing to the weak reducing capacity of the  $\text{H}_2$  environment, the oxygen vacancy concentration of the LBCO thin film under  $\text{H}_2$  is much lower than that found for  $\text{LaBaCo}_2\text{O}_{4.25}$ . Thus, as shown in **Fig. 5**, it is probable that, in the LBCO thin films under  $\text{H}_2$ ,  $\text{CoO}_4$  tetrahedra or square planes are not present, but  $\text{CoO}_5$  square pyramids are. Obviously, the expansion and contraction of the LBCO thin films would be much less for the change between  $\text{CoO}_5$  square pyramids and  $\text{CoO}_6$  octahedra than between  $\text{CoO}_4$  tetrahedra/square-planes and  $\text{CoO}_6$  octahedra.

### 3.5. Chemical dynamics analysis

From the perspective of the  $dR/dt$  vs.  $t$  curves, the LBCO thin films possess ultrafast chemical dynamics during the oxidation cycle, with largest change above  $10^7 \Omega/\text{s}$  even at 300 °C, as shown in **Fig. 4(b)**. In particular, the oxidation reaction (4) at 300 °C has a very short reaction time and a greater change in  $dR/dt$  than does the oxidation reaction (2) at either 300 °C or 500 °C. The ultrafast oxidation from  $\text{Co}^{2+}$  to  $\text{Co}^{3+}$  can be understood as arising from the higher oxygen vacancy concentration and higher reducibility of the LBCO thin films with  $\text{Co}^{2+}$ .

To further understand the dynamic nature of the ultrafast oxidation from  $\text{Co}^{2+}$  to  $\text{Co}^{3+}$ , our data were analyzed by employing the Avrami equation.<sup>35</sup> For a solid-state phase

transformation, the degree of its completion is defined as the volume fraction  $f$  of a new phase in solid phase. A solid-gas reaction consists of several steps such as the adsorption of gaseous molecules on the surface of solid, the dissociation of the molecules, and the atomic diffusion and nucleation, with the rate of the reaction determined by the slowest step. The volume fraction  $f$  as a function of the reaction time can be expressed as

$$f(t) = 1 - \exp[-(t/\tau)^n] \quad (5)$$

where  $f(t)$  is the volume fraction,  $n$  the nucleation factor representing the nucleation type, and  $\tau$  the time for which  $f(t) = 0$ . Normally,  $n = 4$  when nucleation occurs at a constant nucleation rate,  $n = 3$  if the transformation is only the three-dimensional growth of the nuclei after the preformation of the nuclei,  $n = 3 - 4$  if the nucleation rate decreases with time, and  $n > 4$  if the nucleation rate increases with time. For the solid reaction dynamics, it is common to use the resistance change to calculate the volume fraction  $f(t)$  as

$$f(t) = \frac{R_t - R_0}{R_1 - R_0} \quad (6)$$

where  $R_t$ ,  $R_0$ , and  $R_1$  are the resistances of the solid at time  $t$ , at the start ( $t = 0$ ) and at the end of the reaction, respectively. For the oxidation reaction from  $\text{Co}^{2+}$  to  $\text{Co}^{3+}$ , the resistance increases from  $R_{\min}$  to  $R_{\max}$ . Thus, by using equation (5) and (6), the resistance at time  $t$  can be expressed as

$$R = R_{\max} - (R_{\max} - R_{\min}) \exp[-(t/\tau)^n] \quad (7)$$

The analysis of our data using the equation (7) indicates that the oxidation reaction at 300 °C is controlled by the nucleation rate, and the whole reaction can be completed in 3 seconds, as shown in **Fig. 4(c)**.

The phase transition involving the change from the oxidation state  $\text{Co}^{2+}$  to  $\text{Co}^{3+}$  is highly

dependent upon the oxidation temperature. The time constants and the nucleation factors obtained by fitting the resistance curves with the equation (7) are plotted in **Fig. 6**. The reaction rate for the transition from  $\text{Co}^{2+}$  to  $\text{Co}^{3+}$  increases with increasing the temperature (from 260 to 350 °C). From the curve of  $n$  we can find that the nucleation type also varies entirely with temperature. The extraordinary values of  $n \gg 4$  signify that a large numbers of oxygen vacancy sites, which act as potential oxidation nucleation centers, are generated during the reduction process above 300 °C. At 280 °C, nucleation occurs only at the start of the transformation. At 260 °C, the oxidation process from  $\text{Co}^{2+}$  to  $\text{Co}^{3+}$  is reduced in reaction rate and is not nucleation-controlled any longer.

#### 4. Conclusions

The redox dynamics of the epitaxial LBCO thin films exposed to the switching flow of  $\text{H}_2$  and  $\text{O}_2$  gases at 260 – 700 °C were systematically studied by ac resistance measurements. At medium temperatures (400~700 °C), the LBCO thin films are sensitive to the reducing/oxidizing environments, exhibiting a conducting-to-insulating transition in each oxidation/redox cycle. At low temperatures (260~350 °C) under  $\text{H}_2$  environment, the LBCO thin films undergo a conducting-to-insulating-to-conducting transition, which corresponds to the variation of the oxidation states,  $\text{Co}^{4+}/\text{Co}^{3+}$  to  $\text{Co}^{3+}$  to  $\text{Co}^{3+}/\text{Co}^{2+}$ . The oxidation reaction from  $\text{Co}^{2+}$  to  $\text{Co}^{3+}$  at low temperatures is faster than that from  $\text{Co}^{3+}$  to  $\text{Co}^{4+}$ . The time required to change from the  $\text{Co}^{2+}$  to  $\text{Co}^{3+}$  state decreases from 30 to 3 s with increasing the temperature from 260 to 350 °C. The nucleation rate of the reaction at 300 and 350 °C increases with time during their very short reaction process. The ultrafast redox reactions at

300 – 700 °C indicates that the epitaxial LBCO thin films are a promising candidate for low-temperature SOFC cathodes, chemical gas sensors, effective deoxidizers, and vehicle exhaust catalysts.

### **Acknowledgements**

This research was partially supported by the Department of Energy under DE-FE0003780 and the National Science Foundation under NSF-NIRT-0709293 and NSF-PREM DMR-0934218. Also, HBW, SYB, CRM, ML would like to acknowledge the support from the “China Scholarship Council” for the program of national study-abroad project for the postgraduates of high level universities at UTSA.

### Figure Captions

Fig. 1. (a) R vs. t and (b) dR/dt vs. t curves measured for the LBCO thin films under oxidizing/reducing atmospheres at 500 °C.

Fig. 2. Resistance changes vs. the gas flow time, R vs. t, of an epitaxial LBCO thin film: (a) During the reduction (under H<sub>2</sub>) cycle at various temperatures. (b) During the oxidation (under O<sub>2</sub>) cycle at various temperatures.

Fig. 3. (a) R vs. t and (b) dR/dt vs. t curves measured for the LBCO thin films under oxidizing/reducing atmospheres measured at 350°C. (c) A zoomed-in view of the R vs. t curve for one oxidation/reduction cycle showing the variation of the Co oxidation state as a function of t. The dR/dt vs. t curves for the (d) reduction and (e) oxidation processes of the reduction/oxidation cycle presented in (c).

Fig. 4. Redox reactions of the LBCO thin films under the switching flow of reducing/oxidizing gas flow at 300 °C: (a) R vs. t and (b) dR/dt vs. t curves. (c) Avrami analysis of the oxidation reactions associated with the oxidation state change from Co<sup>2+</sup> to Co<sup>3+</sup>.

Fig. 5. Polyhedral representations of the crystal structures of LaBaCo<sub>2</sub>O<sub>6</sub>, LaBaCo<sub>2</sub>O<sub>5.5</sub> and LaBaCo<sub>2</sub>O<sub>5</sub>.

Fig. 6 The n and τ values obtained from the Avrami analysis for the oxidation reactions associated with the change in the Co oxidation state Co<sup>2+</sup> to Co<sup>3+</sup> at temperatures between 260 – 350 °C.

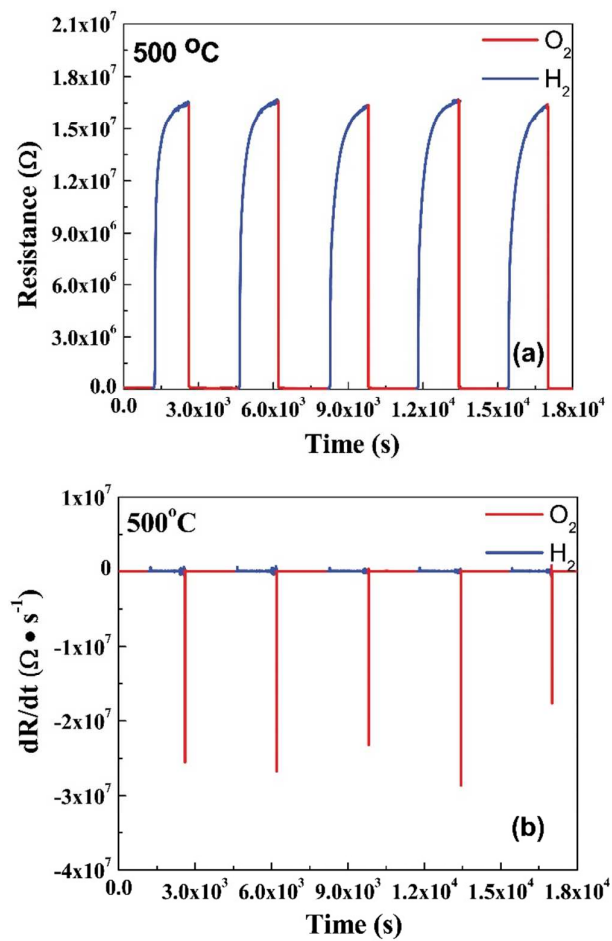


Fig. 1



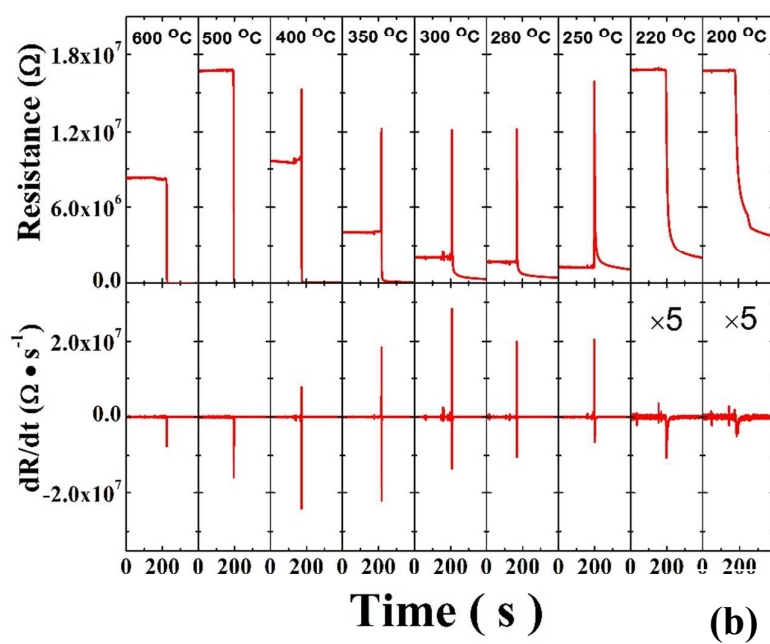
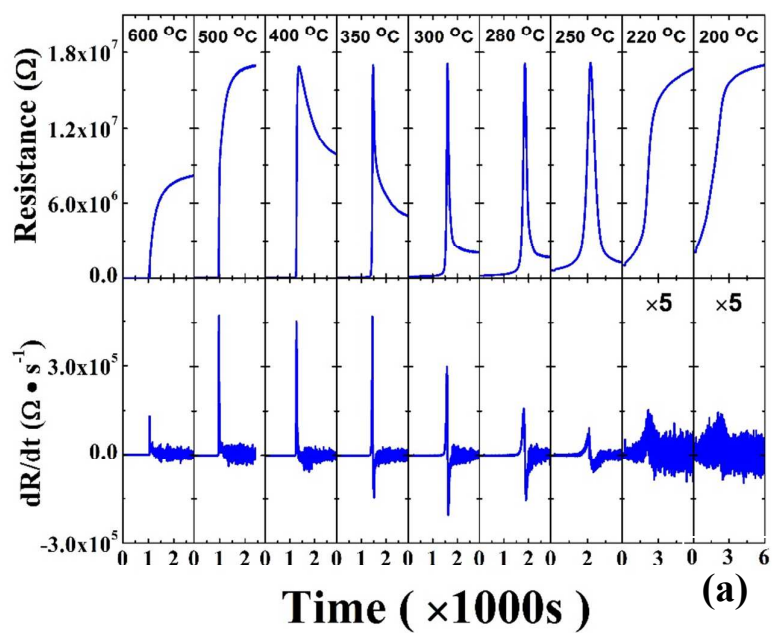


Figure 2

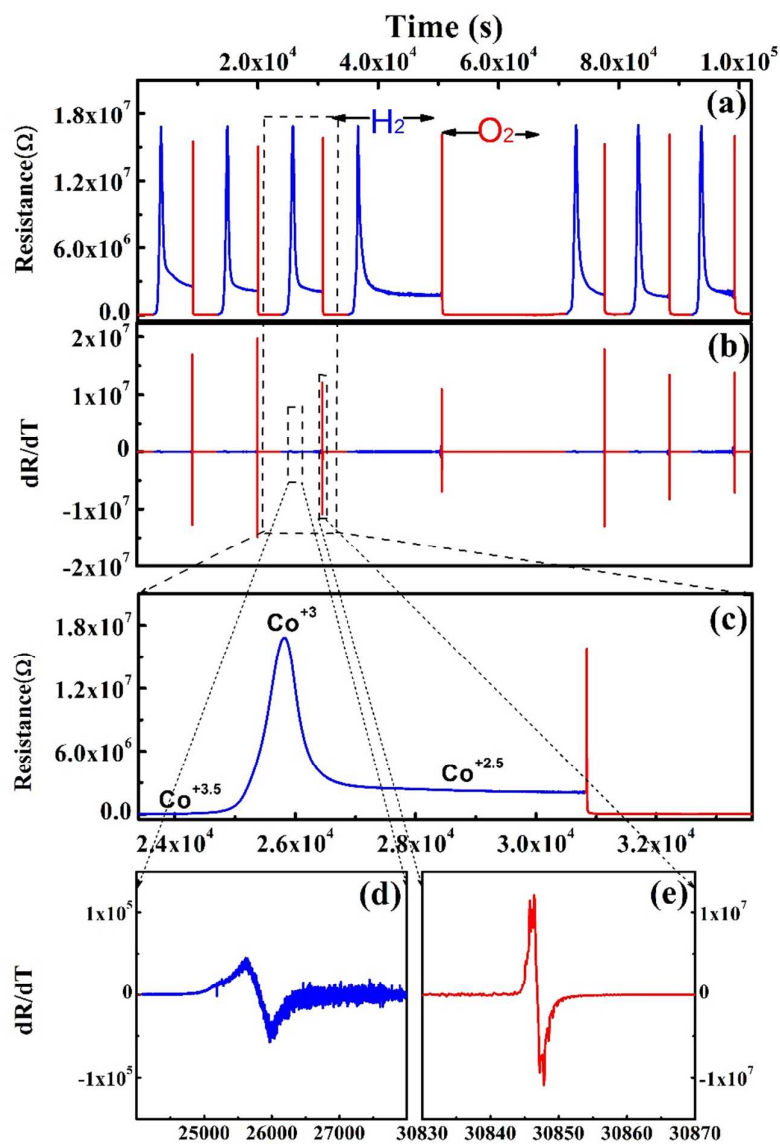


Fig. 3

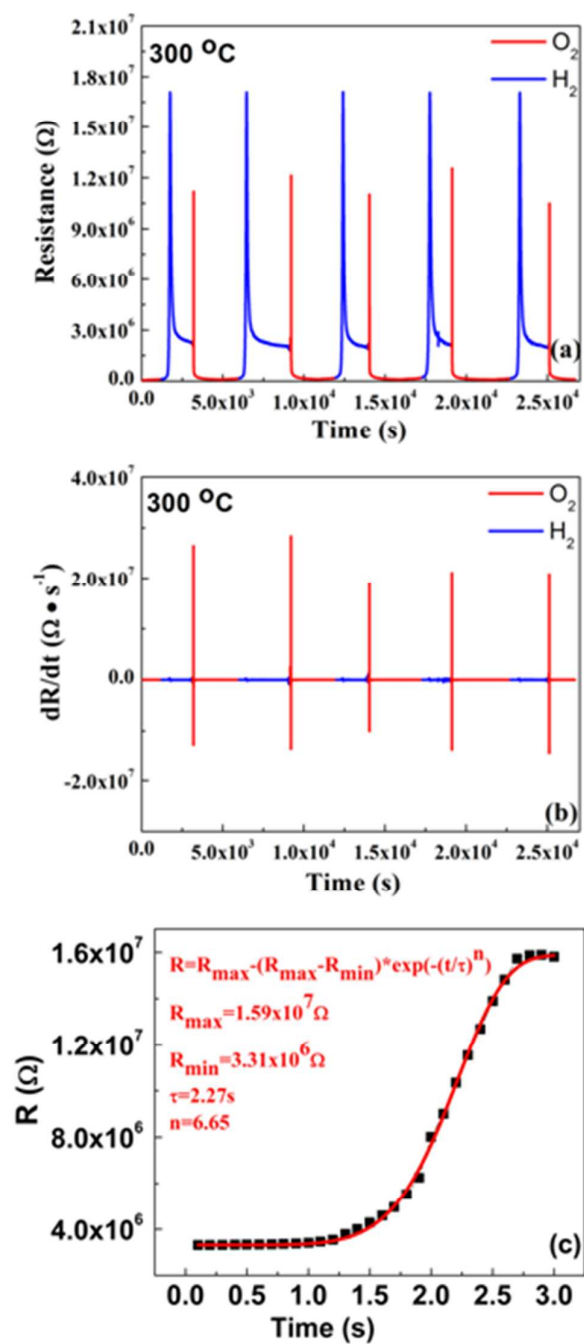


Fig. 4

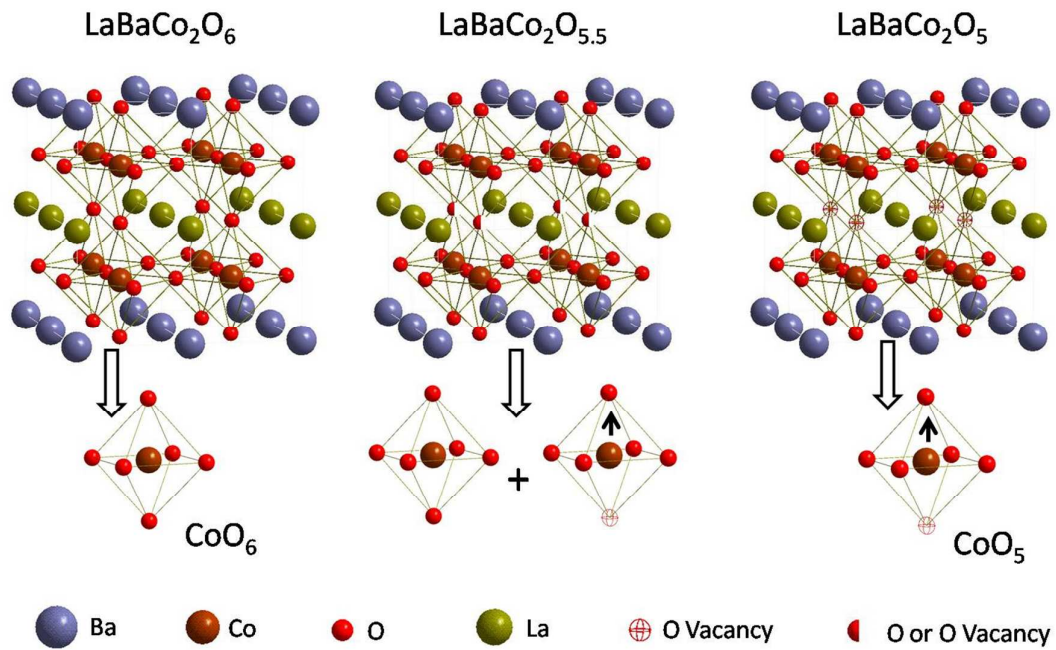


Fig. 5

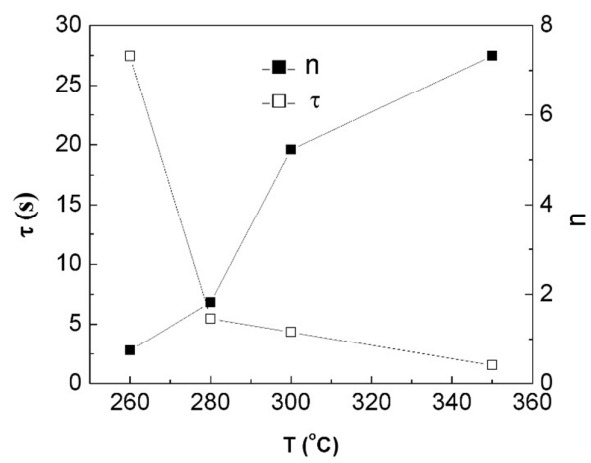


Fig. 6

- 
- <sup>1</sup> S. Roy, I. S. Dubenko, M. Khan, E. M. Condon, J. Craig, N. Ali, W. Liu and B. S. Mitchell, *Phys. Rev. B*, 2005, **71**, 024419.
- <sup>2</sup> A. Maignan, V. Caignaert, B. Raveau, D. Khomskii, and G. Sawatzky, *Phys. Rev. Lett.*, 2004, **93**, 026401.
- <sup>3</sup> T. Hibino, A. Hashimoto, T. Inoue, J.-i. Tokuno, S.-i. Yoshida and M. Sano, *Science*, 2000, **288**, 2031.
- <sup>4</sup> V. V. Kharton, S. B. Li, A. V. Kovalevsky, A. P. Viskup, E. N. Naumovich and A. A. Tonoyan, *Mater. Chem. Phys.*, 1998, **53**, 6.
- <sup>5</sup> N. P. Brandon, S. Skinner and B. C. H. Steele, *Annu. Rev. Mater. Res.*, 2003, **33**, 183.
- <sup>6</sup> A. Tarancón, A. Morata, G. Dezanneau, S. J. Skinner, J. A. Kilner, S. Estradé, F. Hernández-Ramírez, F. Peiró and J. R. Morante, *J. Power Sources*, 2007, **174**, 255.
- <sup>7</sup> A. Tarancon, S. J. Skinner, R. J. Chater, F. Hernandez-Ramirez and J. A. Kilner, *J. Mater. Chem.*, 2007, **17**, 3175.
- <sup>8</sup> A. Chang, S. J. Skinner and J. A. Kilner, *Solid State Ionics*, 2006, **177**, 2009.
- <sup>9</sup> N. Li, Z. Lü, B. Wei, X. Huang, K. Chen, Y. Zhang and W. Su, *J. Alloys Compd.*, 2008, **454**, 274.
- <sup>10</sup> C. Frontera, A. Caneiro, A. E. Carrillo, J. Oró-Solé and J. L. García-Muñoz, *Chem. Mater.*, 2005, **17**, 5439.
- <sup>11</sup> A. A. Taskin, A. N. Lavrov and Y. Ando, *Appl. Phys. Lett.*, 2005, **86**, 091910.
- <sup>12</sup> G. Kim, S. Wang, A. J. Jacobson, L. Reimus, P. Brodersen and C. A. Mims, *J. Mater. Chem.*, 2007, **17**, 2500.
- <sup>13</sup> G. Kim, S. Wang, A. J. Jacobson, Z. Yuan, W. Donner, C. L. Chen, L. Reimus, P. Brodersen and C. A. Mims, *Appl. Phys. Lett.*, 2006, **88**, 024103.
- <sup>14</sup> J. Liu, G. Collins, M. Liu, C. L. Chen, J. He, J. C. Jiang, and E. I. Meletis, *Appl. Phys. Lett.*, 2012, **100**, 193903.
- <sup>15</sup> E.-L. Rautama, P. Boullay, A. K. Kundu, V. Caignaert, V. Pralong, M. Karppinen and B. Raveau, *Chem. Mater.*, 2008, **20**, 2742.
- <sup>16</sup> E.-L. Rautama, V. Caignaert, P. Boullay, A. K. Kundu, V. Pralong, M. Karppinen, C. Ritter and B. Raveau, *Chem. Mater.*, 2008, **21**, 102.

- <sup>17</sup> I. O. Troyanchuk, D. V. Karpinsky, M. V. Bushinsky, V. Sikolenko, V. Efimov and A. Cervellino, *Jetp Lett.*, 2011, **93**, 139.
- <sup>18</sup> A. Maignan, C. Martin, D. Pelloquin, N. Nguyen and B. Raveau, *J. Solid State Chem.*, 1999, **142**, 247.
- <sup>19</sup> J. Seddon, E. Suard and M. A. Hayward, *J. Am. Chem. Soc.*, 2010, **132**, 2802.
- <sup>20</sup> J. Liu, M. Liu, G. Collins, C. L. Chen, X. N. Jiang, W. Gong, A. J. Jacobson, J. He, J. C. Jiang and E. I. Meletis, *Chem. Mater.*, 2010, **22**, 799.
- <sup>21</sup> J. Liu, G. Collins, M. Liu, C. L. Chen, J. Jiang, E. I. Meletis, Q. Zhang and C. Dong, *Appl. Phys. Lett.*, 2010, **97**, 094101.
- <sup>22</sup> M. Liu, J. Liu, G. Collins, C. R. Ma, C. L. Chen, J. He, J. C. Jiang, E. I. Meletis, A. J. Jacobson and Q. Y. Zhang, *Appl. Phys. Lett.*, 2010, **96**, 132106.
- <sup>23</sup> M. Liu, C. R. Ma, J. Liu, G. Collins, C. L. Chen, J. He, J. C. Jiang, E. I. Meletis, L. Sun, A. J. Jacobson and M.-H. Whangbo, *Appl. Mater. Interfaces*, 2012, **4**, 5524.
- <sup>24</sup> J. He, J. C. Jiang, J. Liu, M. Liu, G. Collins, C. R. Ma, C. L. Chen and E. I. Meletis, *Thin Solid Films*, 2011, **519**, 4371.
- <sup>25</sup> C. R. Ma, M. Liu, G. Collins, J. Liu, Y. M. Zhang, C. L. Chen, J. He, J. C. Jiang and E. I. Meletis, *Appl. Phys. Lett.*, 2012, **101**, 021602.
- <sup>26</sup> C. R. Ma, M. Liu, G. Collins, H. B. Wang, S. Y. Bao, X. Xu, E. Enriquez, C. L. Chen, Y. Lin and M.-H. Whangbo, *Appl. Mater. Interfaces*, 2012, **5**, 451.
- <sup>27</sup> Z. Yuan, J. Liu, C. L. Chen, C. H. Wang, X. G. Luo, X. H. Chen, G. T. Kim, D. X. Huang, S. S. Wang, A. J. Jacobson, and W. Donner, *Appl. Phys. Lett.*, 2007, **90**, 212111.
- <sup>28</sup> J. Liu, G. Collins, M. Liu, and C. L. Chen, *APL Mat* 2013, **1**, 031101
- <sup>29</sup> S. Y. Bao, C. R. Ma, G. Chen, X. Xu, E. Enriquez, C. L. Chen, Y. M. Zhang, J. L. Bettis, M.-H. Whangbo, C. Dong and Q. Y. Zhang, *Sci. Rep.*(in press).
- <sup>30</sup> D. Emin and T. Holstein. *Ann. Phys.*, 1969, **53**, 439.
- <sup>31</sup> S. Mollah, H. L. Huang, H. D. Yang, S. Pal, S. Taran and B. K. Chaudhuri, *J. Magn. Magn. Mater.*, 2004, **284**, 383.
- <sup>32</sup> X. J. Chen, C. L. Zhang, C. C. Almasan, J. S. Gardner and J. L. Sarrao, *Phys. Rev. B*, 2003, **67**, 094426.
- <sup>33</sup> T. Koslowski, *Phys. Chem. Chem. Phys.*, 1999, **1**, 3017.

---

<sup>34</sup> M. Olette and M. F. Ancey-Moret, *Rev. Mét.*, 1963, **60**, 569.

<sup>35</sup> M. Avrami, *J. Chem. Phys.*, 1939, **7**, 1103.